

Original Article

Assessment of the Accuracy, Precision and Reproducibility of Apparent Diffusion Coefficient Measurements on a Clinical Magnetic Resonance Imaging System

Sadegh Shurche¹, Nader Riahi Alam^{2*}

1- MSc Student, Physics and Medical Engineering Department, Medical Faculty, Tehran University of Medical Sciences, Tehran, Iran.

2- Professor, Physics and Medical Engineering Department, Medical Faculty, Tehran University of Medical Sciences, Tehran, Iran.

Received:4 June 2017

Accepted:25 August 2017

Keywords:

Diffusion-Weighted MRI;
Tissue-Equivalent Diffusivity
Material; Diffusion Phantom;
Quality Control.

ABSTRACT

Purpose- The purpose of this work was to investigate a quality control protocol for 1.5 T clinical MRI system on tissue-equivalent diffusivity phantoms made of Nickel-doped agarose/sucrose gels.

Materials and Methods- We designed and manufactured a spherical phantom using these gels for T_1 , T_2 and DW-MRI. Every compartments was filled with tissue equivalent relaxation and diffusivity gels. After that we assessed the quality control protocol for T_1 , T_2 and DW-MRI on these gels and the magnetic resonance imaging of the phantom was performed on the 1.5 T clinical MRI system IMAM KHOMEINI hospital of TEHRAN (GE GENESIS SIGNA). Two parameters, Q and R , are used for the analysis of the quality control ADC values.

Results- T_2 gel values, 84.804 ± 3 , 80.773 ± 2 , 86.57 ± 2 , 77.774 ± 13 , 77 ± 2 (ms), were respectively obtained for BT(body tissue), P2(tumor), P2 in air, P2 in oil, P1(ischemi). Also, their corresponding T_1 measurements were 1090.92 ± 3 , 1742.75 ± 4 , 1284.75 ± 3 , 1400 ± 11 , 1358.23 ± 3 (ms) respectively. Using this phantom DW- MRI experiments can be performed under very realistic conditions. The Q calculated for the P1 and P2 in different b-values (150, 400, 1000 $\text{mm}^2 \text{s}^{-2}$) is smaller than the Q for BT. This observation is likely to indicate that for b-values 150, 400, 1000 $\text{mm}^2 \text{s}^{-2}$, the ADC measurement reproducibility is compromised by ADC deviations due to the difference between effective and nominal b-values over time. The R parameter used in our quality control protocol to quantitatively study the directional dependence is expected to be governed by the ADC fluctuation described by the equation of measurement of differences between nominal and effective b-values.

Conclusion- The quality control protocol presented in this study will be valuable for monitoring the diffusion imaging performance of an MRI system in a clinically relevant way.

1. Introduction

Diffusion-Weighted Magnetic Resonance Imaging (DW-MRI) scan is typically used to diagnose stroke in a timely manner [1]. This

type of imaging can be used to scan tumors in various parts of the body [2]. Apparent Diffusion Coefficient (ADC) is a tissue specific parameter, which is used for the evaluation of the tumor response to therapy.

***Corresponding Author:**

Nader Riyahi-Alam, PhD

Physics and medical engineering Department, Medical Faculty, Tehran University of Medical Sciences, P.O.Box: 14176-13151, Tehran, Iran.

Tel: (+98)2166466383.

Email: riahialam@gmail.com

Diffusion-weighted imaging plays an important role in the management of cancer treatment [3].

Tissue-equivalent phantoms with diffusivity property have an important role in implementing the quality control of the existing and new protocols of the diffusion-weighted imaging.

Materials and test objects suitable for MRI diffusion measurements have been described before [4]. Ioannis Delakis *et al.* developed a quality control protocol on two aqueous test solutions of CuSO_4 and sucrose [4]. ADC measurement with the CuSO_4 solution is more sensitive to differences between nominal and effective b-values, on the account of the solution's high ADC. ADC measurement with the sucrose solution is more sensitive to signal reproducibility due to the solution's low baseline signal intensity. Analysis with the Q parameter indicates that signal reproducibility errors contribute to ADC variations on their MRI system when imaging with high b-values ($b > 500 \text{ mm s}^{-2}$), whereas differences between nominal and effective b-values have a greater impact on the ADC measurement when imaging with low b-values ($b < 500 \text{ mm s}^{-2}$). Analysis with the R parameter shows that the effect of directional variation of the ADC measurement on our MRI system is more pronounced when imaging with low b-values. Therefore, it must be notified that any component used must have relaxation and diffusion properties similar to the ones found in healthy or malignant biological tissues. To our knowledge, an independent control of T_1 , T_2 and ADC within a single substance might have not been demonstrated yet [5]. However, a series of gels can control the relaxation and diffusion properties independently. Recently, Lavdas *et al.* have reported a nickel-doped agarose/sucrose gels that can be used as reference materials for MRI diffusion measurements [6]. By altering the concentration of each chemical component in the nickel-doped agarose/sucrose gels, one can control the relaxation and diffusion properties almost independently. These gels had relaxation and diffusion properties similar to healthy or malignant biological tissues, easy to produce in a reproducible manner and they are made of inexpensive and commonly available materials. Furthermore, the gels are nontoxic and are easy and safe to store and transport.

The purpose of our work was to investigate a diffusion imaging quality control protocol for 1.5 T clinical MRI system on tissue-equivalent diffusivity phantoms made of nickel-doped agarose/sucrose gels previously manufactured by Ioannis Lavdas *et al.* Also in our previous article [7], we started to build this phantom and the quality control of the 3 Tesla system and in the following we designed and manufactured a spherical phantom using these gels for T_1 , T_2 and DW-MRI. Every compartments was filled with tissue-equivalent relaxation and diffusivity gels. After that, we assessed the delakis [4] quality control protocol for T_1 , T_2 and DW-MRI on these gels.

2. Materials and Methods

2.1. Nickel-Doped Agarose/Sucrose Gels

To assess the quality control, we prepared nickel-doped agarose/sucrose gels according to literature [6].

The relaxation and diffusion properties of the 3 gels were measured on a 1.5 T clinical system using the methods described in the appropriate section.

2.2. Diffusion Phantom

To perform a quality control on MRI protocols, we designed a spherical phantom by solid work software in accordance with lecture [6].

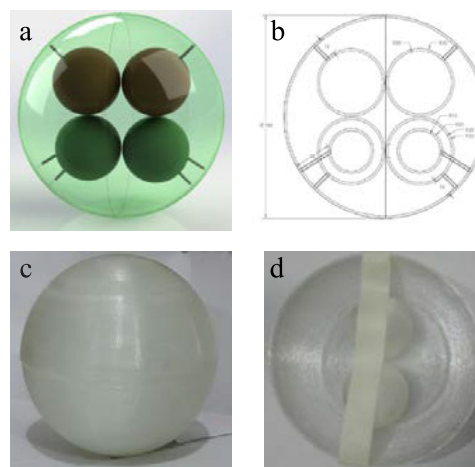


Figure 1. a) The designed phantom by solid work software. b) Internal pattern of phantom. c) The external pattern of phantom manufactured by 3D printer. d) The internal pattern of phantom manufactured by 3D printer.

2.3. MRI and Quantitative Image Analysis

The quality control protocol was applied on a 1.5 T clinical MRI system at IMAM KHOMEINI hospital of TEHRAN (GE GENESIS SIGNA), using a circularly polarized 2 channel head coil in receive mode in 1.5 T. The test object was placed within head coil and left in the magnet bore a few minutes prior to scanning. After that, the relaxation and diffusion properties (T_1 , T_2 , and ADC) of the gels were measured.

The measurement methods used has been described here. A Spin Echo (SE) pulse sequence with the following parameters was used for T_1 and T_2 measurements in 1.5 T: Field of View (FOV) $\frac{1}{4}$ 250 _ 250 mm, matrix size $\frac{1}{4}$ 256 _ 256, number of averages NA $\frac{1}{4}$ 1, image bandwidth $\frac{1}{4}$ 320 Hz/pixel, slice thickness $\frac{1}{4}$ 5 mm, number of slices $\frac{1}{4}$ 1. For the T_1 measurements, seven Repetition Time (TR) values were used (100, 300, 700, 1000, 1500, 2200, 3500 ms) with an Echo Time (TE) of 11 ms and for the T_2 measurements, 10 TE values were used (30- 120 ms in steps of 10 ms) with a TR of 3000 ms.

DW-MRI was performed using a single-shot EPI pulse sequence with the following parameters: FOV $\frac{1}{4}$ 250* 250 mm, matrix size $\frac{1}{4}$ 256* 256, TR $\frac{1}{4}$ 4000 ms, TE $\frac{1}{4}$ 62.2 ms, NA $\frac{1}{4}$ 4, image bandwidth $\frac{1}{4}$ 320 Hz/pixel, GRAPPA factor 2, reference lines $\frac{1}{4}$ 46, SPAIR fat suppression, slicethickness $\frac{1}{4}$ 5 mm, number of slices $\frac{1}{4}$ 6, zeroslice gap and distance factor. Three b-values were used: 150, 400, and 1000 s/mm². It is important to mention that the b-values used in the diffusion pulse sequence did not allow the diffusion-weighted signal to approach the background noise intensity level.

We defined two parameters Q and R for quality control, and we performed our calculations based on the formulas expressed in the appendix for these two parameters. Also, for calculating the ADC, the formula was used in the appendix.

Diffusion sensitization was applied independently along the three orthogonal directions: Superior–Inferior (SI), Anterior–Posterior (AP) and Right–Left (RL). The three respective directional ADC images, ADC_{SI} , ADC_{AP} and ADC_{RL} were then calculated using an independent platform. A fourth image, the trace ADC (ADC_T) was also calculated as the average of the directional ADC images.

T_1 , T_2 and ADC maps were generated in MIPAV image processing software (Medical Image Processing, Analysis and Visualization, National Institutes of Health, Bethesda, MD). Region Of Interest (ROIs) were drawn on the center of each phantom compartment to calculate the average T_1 , T_2 , and ADC values. ADC quality control parameters was assessed according to three orthogonal directions.

3. Result

3.1. Relaxation and Diffusion Properties of the Gels Within the Spherical Phantom

To calculate average T_1 , T_2 , and ADC values, ROIs were drawn in the center of each compartment, avoiding artifacts regions. For the “BT” compartment, five ROIs were drawn throughout the whole compartment and were grouped before the calculating the average T_1 , T_2 , and ADC values.

T_1 , T_2 and ADC maps were generated for the spherical phantom using the methods described in the relevant section and are shown in the Figure 2.

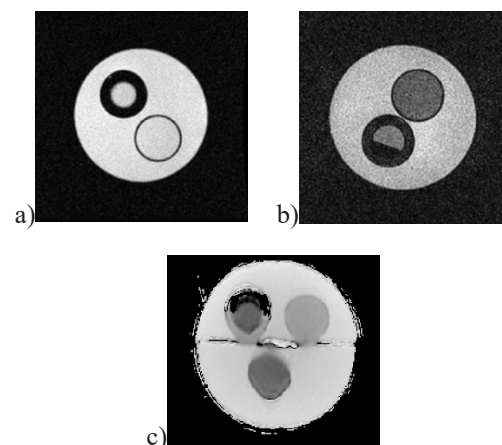
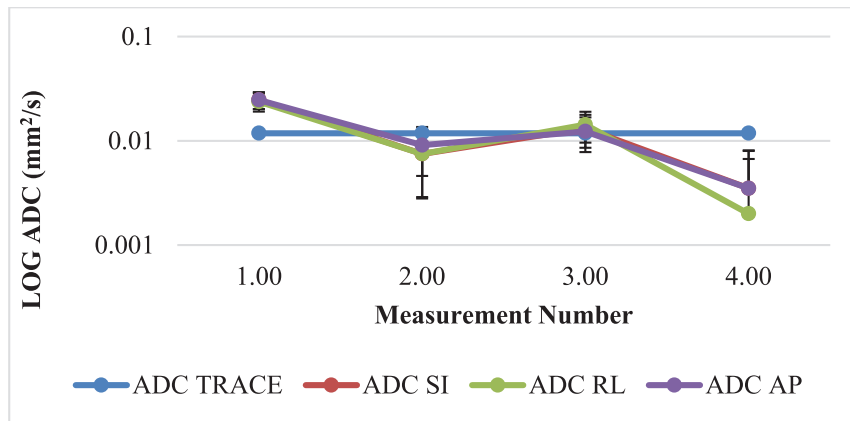
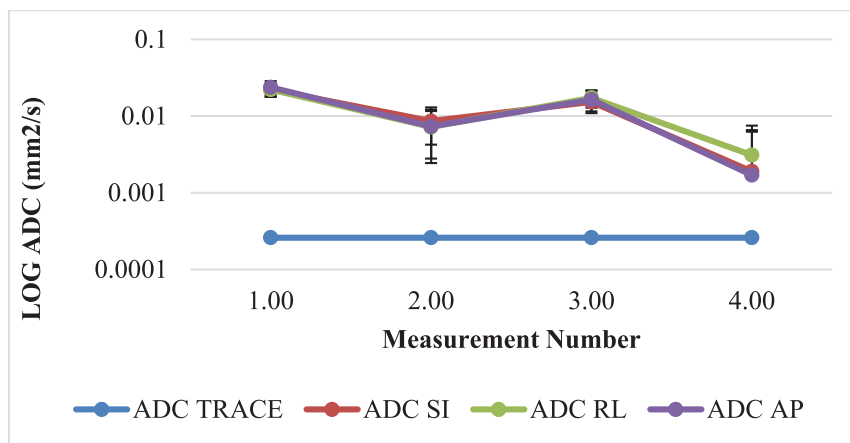


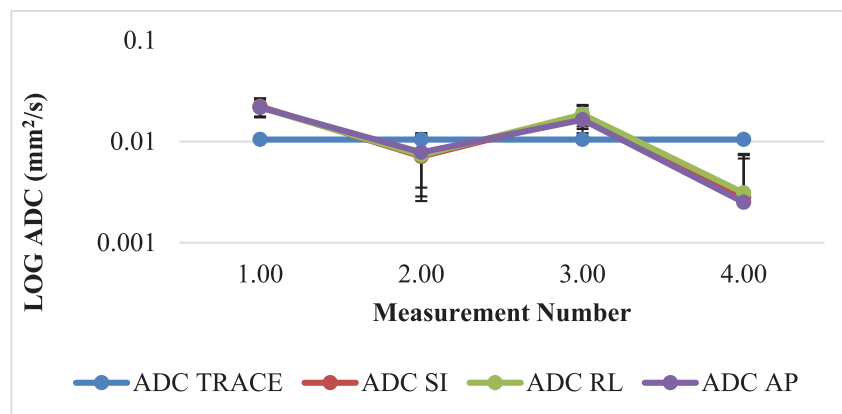
Figure 2. a) T_1 . b) T_2 . c) ADC map. The reason for the distortion artifacts of diffusion images is the defect in the device gradients.



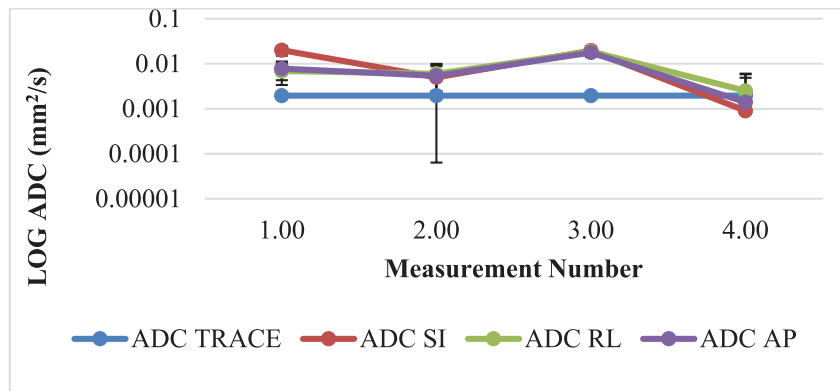
(a)



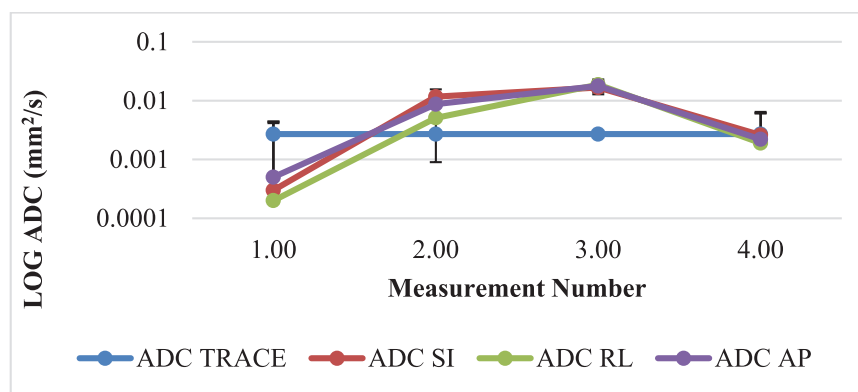
(b)



(c)



(d)



(e)

Figure 3. ADC values measured with the quality control protocol. relative to ADC_{τ} (straight solid line) of the test object solution. (a) Test solution: BT, b-values: [150,400,1000] mm s⁻², (b) Test solution: P2, b-values: [150,400,1000] mm s⁻², (c) Test solution: P1, b-values: [150,400,1000] mm s⁻², (d) Test solution: P2 in air, b-values: [150,400,1000] mm s⁻², (e) Test solution: P2 in oil, b-values: [150,400,1000] mm s⁻².

The measured relaxation times of the gels within the phantom compartments was shown in Table 1.

The ADC_T values of the test object gels employed in the quality control program also are shown in Table 2.

Table 2. The T₁ and T₂ results from different signal intensity in comparison with different repetition time (TR) and ADC_T and δ(ADC_T) of the test object solutions employed in the quality control programme in 1.5 T.

GEL	b-value (mm ² s ⁻²)	ADC _T (×10 ⁻³ mm ² s ⁻¹)	δ(× 10 ⁻³ ADC _T) (mm ² s ⁻¹)	T ₁ (ms)	T ₂ (ms)
BT	150	25 ± 0.001	3	1090.92 ± 3	84.804± 3
	400	8 ± 0.001	0.29		
	1000	3 ± 0.002	0.30		
P2	150	2 ± 0.001	0.14	1742.75 ± 4	80.773± 2
	400	7 ± 0.001	0.50		
	1000	2 ± 0.002	0.14		
P1	150	21 ± 0.001	2.5	1358.23 ± 3	77 ± 2
	400	7.4 ± 0.001	0.26		
	1000	2.1 ± 0.001	0.14		
P2 IN AIR	150	2.1 ± 0.002	0.14	1284.75± 3	86.57 ± 2
	400	2.1 ± 0.001	0.14		
	1000	1.6 ± 0.002	0.13		
P2 IN OIL	150	0.2 ± 0.0001	0.11	1400 ± 11	77.774± 13
	400	5 ± 0.002	0.21		
	1000	2 ± 0.001	0.14		

The ADC_{SI}, ADC_{AP}, ADC_{RL} and ADC_T values acquired from the quality control protocol are displayed in Table 3 for each combination of

solution and b-value. Table 3 lists the results from the analysis of the quality control data with the R parameter.

Table 3. Mean directional and R parameter results from the analysis of the quality control protocol ADC values for each combination of test solution and b-value.

GEL	b-value(mm.s ⁻²)	Mean ADC _{SI} (×10 ⁻³)	Mean ADC _{RL} (×10 ⁻³)	Mean ADC _{AP}	Mean R
BT	150	20 ± 0.01	20 ± 0.01	20 ± 0.01	3.3 ± 0.01
	400	7 ± 0.002	7 ± 0.01	9 ± 0.002	7 ± 0.1
	1000	3 ± 0.001	2 ± 0.02	3 ± 0.001	10.3 ± 0.1
P2	150	20 ± 0.02	20 ± 0.01	20 ± 0.02	5.77 ± 0.1
	400	8 ± 0.001	7 ± 0.002	7 ± 0.001	6.9 ± 0.1
	1000	1 ± 0.002	3 ± 0.001	1 ± 0.001	9.7 ± 0.2
P1	150	20 ± 0.01	20 ± 0.01	20 ± 0.01	4.5 ± 0.1
	400	7 ± 0.001	7 ± 0.001	7 ± 0.002	6.4 ± 0.2
	1000	2 ± 0.002	2 ± 0.001	2 ± 0.001	12.4 ± 0.1
P ₁ IN AIR	150	20 ± 0.01	6 ± 0.001	7 ± 0.002	5.8 ± 0.2
	400	5 ± 0.001	6 ± 0.001	5 ± 0.001	7.9 ± 0.1
	1000	0.9 ± 0.0001	2 ± 0.002	1 ± 0.001	13.9 ± 0.1
P ₂ IN OIL	150	0.3 ± 0.0001	0.2 ± 0.0001	0.5 ± 0.0002	4 ± 0.2
	400	10 ± 0.02	5 ± 0.001	8 ± 0.001	4.3 ± 0.2
	1000	2 ± 0.001	1 ± 0.002	2 ± 0.002	9 ± 0.2

The $\delta(\text{ADC}_T)$ used in the calculation of Q and R was the one measured with the test object solutions (see Table 4). The Q parameter was calculated

independently for ADC_{SI} , ADC_{AP} , ADC_{RL} and ADC_T . The Q results presented in Table 4 are for ADC_T .

Table 4. Q parameter results from the analysis of the quality control ADC_T values for each combination of test solution and b-value.

GEL	b-value	SD($\times 10^{-3}\text{ADC}_T$)	SD(ADC_T)/ $\delta(\text{ADC}_T)$	Q
BT	150	2.2	23.00	2 ± 0.1
	400	7.23	24.44	1.9 ± 0.01
	1000	0.42	2.63	2.5 ± 0.1
P2	150	0.34	3.77	0.5 ± 0.01
	400	0.54	2.35	0.5 ± 0.1
	1000	0.34	3.77	1 ± 0.1
P1	150	2.28	1.62	1.5 ± 0.1
	400	0.85	3.16	1.8 ± 0.1
	1000	0.34	3.77	0.5 ± 0.02
P1 IN AIR	150	0.34	3.77	0.5 ± 0.1
	400	0.34	3.77	0.5 ± 0.01
	1000	0.31	2.43	2 ± 0.1
P2 IN OIL	150	0.10	1.19	1.4 ± 0.1
	400	0.91	4.29	1.5 ± 0.1
	1000	0.37	2.53	0.2 ± 0.01

4. Discussion

The T_1 , T_2 and ADC maps in Figure (2) shows the relaxation and diffusion properties of this phantom is similar to the ones found in biological tissues specially in biological tissues such as fat tissue and air tissue boundaries (Table 2). The T_2 of the gels was assessed to be 84.804 ms, 80.773 ms, 77 ms, 86.570 ms, and 77.774 ms for BT, P2, P1, P1 in air, P2 in oil, respectively, with a measurement accuracy of 5%. Their T_1 measurements was 1090.92 ms, 1742.75 ms, 1358.23 ms, 1284.75 ms, and 1400 ms respectively. For comparison, typical T_2 value of white matter is 82 ms, of grey matter is 92 ms, of cerebrospinal fluid is 2280 ms [6, 8], and of tumor is 98 ms. The T_1 values of white matter, grey matter, and cerebrospinal fluid are 1374 ms, 914ms, and 80 ms, respectively. The value of the ADC is characteristic of tissue structure and ranges between 60 and $105 \times 10^{-5} \text{mm}^2\text{s}^{-1}$ in white matter, between 60 and $83 \times 10^{-5} \text{mm}^2\text{s}^{-1}$ in grey matter and between 240 and $440 \times 10^{-5} \text{mm}^2\text{s}^{-1}$ in cerebrospinal fluid [9]. This means that using this phantom DW- MRI experiments can be performed under very realistic conditions.

Thus the specific imaging object can be a valuable assistance for optimizing diffusion protocols, exploring the usefulness of novel pulse sequences for DW-MRI and comparing ADC values between field strengths, vendors and imaging centers.

The Q calculated for the P1 and P2 in different b-values (150, 400, 1000 mm s^{-2}) is smaller than the Q for BT (Table 4). This observation is likely to indicate that for b-values 150, 400, 1000 mm s^{-2} , the ADC measurement reproducibility is compromised by ADC deviations due to the difference between effective and nominal b-values over time. Indeed, the ADC of the BT is greater than the ADC of P1 and P2, reflecting the relationship between their respective Q values.

ADC_{SI} , ADC_{RL} and ADC_{AP} for each compartment for each b-value should be equal, but a small and consistent offset was shown among them in all instances (Table 3). This error is currently taken into account for the analysis of clinical studies employing the diffusion imaging sequence used in this quality control protocol. According to the equation of ADC calculation [10], by increasing

the b-value, the ADC is decreased in all instances (Table 3). Table 3 and Figure 3 presents the results of the ADC quality control dataset analysis with regard to ADC measurement directional dependence. The directional dependence of ADC is likely to be determined by discrepancies between effective and nominal b-values in each direction. Therefore, the R parameter used in our quality control protocol to quantitatively study the directional dependence is expected to be governed by the ADC fluctuation described by the equation of measurement of differences between nominal and effective b-values. In fact, the R is highest for P₂ in oil with b-value of 1000 mm s⁻² and lowest for BT with b-value of 150 mm s⁻² (Table 3), as predicted by the equation of measurement of differences between nominal and effective b-values.

We manufactured nickel-doped agarose/sucrose gels which are used as reference materials for DW-MRI experiments. The gels are made of readily available, cost effective, and nontoxic materials. The relaxation and diffusion properties of these gels is similar to the ones found in healthy or malignant biological tissues. We have used this phantom to successfully optimize a whole-body DW-MRI protocol in our clinical systems and to assess the reproducibility of ADC measurements using this protocol. When avoiding regions of artifacts, the reproducibility of ADC measurements was very good.

An analysis of the results identified differences in the performance of our MRI system depending on the prescribed b-value. The quality control protocol also detected a systematic offset amongst the directional ADC values, which is currently taken into account in the analysis of clinical studies employing the diffusion imaging sequence used in this quality control protocol.

5. Conclusion

The analysis of the precision and accuracy of ADC measurement can be a guideline for future studies and for the evaluation of other potential test-object materials. The b-values of the diffusion imaging quality control pulse sequence can be applied on most clinical MRI systems supporting diffusion imaging and the proposed test object solutions can be easily and inexpensively prepared.

As diffusion imaging becomes commonly available on clinical MRI scanners, the quality control protocol presented in this study will be of value for monitoring the diffusion imaging performance of an MRI system in a clinically relevant way. It is important to point out that in the case of in vivo MRI diffusion studies, the patient motion and physiological processes may have a more decisive effect on the accuracy and precision of ADC measurement than MRI system factors. However, the proposed quality control protocol can identify intrinsic measurement limitations associated with clinical observations.

Acknowledgments

We thank Food and Drug Administration (FDA) Lab of Imam Khomeini hospital in Iran for their contributions to this project.

Reference

- 1- S. Warach, et al., Fast magnetic resonance diffusion-weighted imaging of acute human stroke. *Neurology*, 1992. 42(9): p. 1717-1717.
- 2- T. Takahara, Y. Imai, T. Yamashita, S. Yasuda, S. Nasu, and M. Van Cauteren, "Diffusion weighted whole body imaging with background body signal suppression (DWIBS): technical improvement using free breathing, STIR and high resolution 3D display," *Matrix*, vol. 160, no. 160, p. 160, 2004.
- 3- A. R. Padhani et al., "Diffusion-weighted magnetic resonance imaging as a cancer biomarker: consensus and recommendations," *Neoplasia*, vol. 11, no. 2, pp. 102-125, 2009.
- 4- I. Delakis, E. M. Moore, M. O. Leach, and J. P. De Wilde, "Developing a quality control protocol for diffusion imaging on a clinical MRI system," *Physics in medicine and biology*, vol. 49, no. 8, p. 1409, 2004.
- 5- H. Laubach et al., "A Phantom for diffusion-weighted imaging of acute stroke," *Journal of Magnetic Resonance Imaging*, vol. 8, no. 6, pp. 1349-1354, 1998.
- 6- I. Lavdas, K. C. Behan, A. Papadaki, D. W. McRobbie, and E. O. Aboagye, "A phantom for diffusion-weighted MRI (DW-MRI)," *Journal of Magnetic Resonance Imaging*, vol. 38, no. 1, pp. 173-179, 2013.
- 7- S. Shurche and N. Riahi Alam, "A Phantom for Diffusion Weighted MRI," *Frontiers in Biomedical Technologies*, vol. 3, no. 1-2, pp. 34-40, 2017.
- 8- A. Pfefferbaum, E. V. Sullivan, M. Hedehus,

M. Moseley, and K. O. Lim, "Brain gray and white matter transverse relaxation time in schizophrenia," *Psychiatry Research: Neuroimaging*, vol. 91, no. 2, pp. 93-100, 1999.

9- C. Pierpaoli, P. Jezzard, P. J. Basser, A. Barnett, and G. Di Chiro, "Diffusion tensor MR imaging of the human brain," *Radiology*, vol. 201, no. 3, pp. 637-648, 1996.

10- E. O. Stejskal and J. E. Tanner, "Spin diffusion measurements: spin echoes in the presence of a time-dependent field gradient," *The journal of chemical physics*, vol. 42, no. 1, pp. 288-292, 1965.

Appendix

a. Derivation of Equation for Calculating ADC

Equation for calculating ADC :

$$ADC = \frac{1}{b} \ln\left(\frac{S_0}{S_b}\right) \quad (1)$$

The ADC measurement from the diffusion-weighted (S_b) and non-diffusion-weighted (S_0) signal acquisitions has been described in Equation 1 and can be re-written as follows:

$$ADC = \frac{1}{b} \ln(S_0) - \frac{1}{b} \ln(S_b) \quad (2)$$

The uncertainties of S_b and S_0 , denoted by $\delta(S_b)$ and $\delta(S_0)$, respectively are equal to the noise level (n) of the signal acquisitions. However, MRI noise is unaffected by diffusion weighting and is therefore equal for S_b and S_0 ,

$$n = \delta(S_0) = \delta(S_b) \quad (3)$$

The uncertainty of the ADC measurement can be expressed as a function of the uncertainties of S_b and S_0 by using error propagation techniques,

$$\delta(ADC) = \sqrt{\left(\frac{\delta ADC}{\delta S_0}\right)^2 \delta(S_0)^2 + \left(\frac{\delta ADC}{\delta S_b}\right)^2 \delta(S_b)^2} \quad (4)$$

By calculating the partial differentiations from Equation 1 and inserting Equation 2 in Equation 3, the $\delta(ADC)$ can be expressed as:

$$\delta(ADC) = \frac{1}{b} \frac{n}{S_0} \sqrt{\left(\frac{S_b}{S_0}\right)^2 + 1} \quad (5)$$

From Equation 1 the ratio S_b of S_0 is equal

$$\frac{S_b}{S_0} = \exp(-b \times ADC) \quad (6)$$

By inserting Equation 5 in Equation 4, the $\delta(ADC)$ can be written as:

$$\delta(ADC) = \frac{\sqrt{1 + [\exp(b \times ADC)]^2} \frac{n}{S_0}}{b} \quad (7)$$

If SNR_0 is the Signal-to-Noise Ratio in the non-diffusion-weighted acquisition, then the $\delta(ADC)$ of Equation 6 is express as:

$$\delta(ADC) = \frac{\sqrt{1 + [\exp(b \times ADC)]^2} \frac{1}{SNR_0}}{b} \quad (8)$$

b. Statistical Theory Used in the Definition of the Q Parameter

Let us assume that we are making several sets of measurements, each containing N individual measurements. According to statistical theory, the uncertainty of the means of these sets of measurements, denoted by δ_m , is given by:

$$\delta_m = \frac{\delta}{\sqrt{N}} \quad (9)$$

where δ is the uncertainty in a single set of N measurements.

In the proposed quality control protocol, the ADC is measured each time as the mean in the 30×30 pixel ROI so that $\delta(ADC)$ is the uncertainty in a set of $N = 900$ measurements. Therefore, the uncertainty $\delta_m(ADC)$ of the ADC values acquired during the quality control protocol is in theory:

$$\delta_m(ADC) = \frac{\delta(ADC)}{\sqrt{N}} \quad (10)$$

However, the standard deviation of the ADC values acquired with the quality control protocol, denoted by $SD(ADC)$, is higher than $\delta_m(ADC)$ because of external factors interfering with the ADC measurement. Therefore, by calculating the ratio of $SD(ADC)$ to $\delta_m(ADC)$, defined as Q, we measure the magnitude of the observed deviation in relation to the statistical uncertainty of the ADC measurement:

$$Q = \frac{SD(ADC)}{\delta(ADC)} = \sqrt{N} \frac{SD(ADC)}{\delta(ADC)} \quad (11)$$

c. Directional Variation of ADC Measurement

In order to study the directional dependence of the ADC measurement, a parameter R was defined as the ratio of the spread of the directional ADC values to the uncertainty $\delta(\text{ADC})$ of the ADC measurement:

$$R = \frac{\max(\text{ADC}_{SI}, \text{ADC}_{RL}, \text{ADC}_{AP}) - \min(\text{ADC}_{SI}, \text{ADC}_{RL}, \text{ADC}_{AP})}{\delta(\text{ADC})} \quad (12)$$

Where $\max(\text{ADC}_{SI}, \text{ADC}_{RL}, \text{ADC}_{AP})$ and $\min(\text{ADC}_{SI}, \text{ADC}_{RL}, \text{ADC}_{AP})$ are functions calculating the maximum and minimum values of their arguments, respectively.